Hydration of Simple Amides. FTIR Spectra of HDO and Theoretical Studies

ARTICLE *in* THE JOURNAL OF PHYSICAL CHEMISTRY B · FEBRUARY 2008

Impact Factor: 3.3 · DOI: 10.1021/jp7099509 · Source: PubMed

6 AUTHORS, INCLUDING:

Aneta Panuszko
Gdansk University of Technology
12 PUBLICATIONS **169** CITATIONS
SEE PROFILE

Maciej Smiechowski
Gdansk University of Technology
25 PUBLICATIONS **287** CITATIONS
SEE PROFILE

Joanna Krakowiak
Gdansk University of Technology
23 PUBLICATIONS **211** CITATIONS
SEE PROFILE

Janusz Stangret
Gdansk University of Technology
37 PUBLICATIONS **611** CITATIONS
SEE PROFILE

Hydration of Simple Amides. FTIR Spectra of HDO and Theoretical Studies

Aneta Panuszko, Emilia Gojło, Jan Zielkiewicz, Maciej Śmiechowski, Joanna Krakowiak, and Janusz Stangret*

Department of Physical Chemistry, Chemical Faculty, Gdańsk University of Technology, Narutowicza 11/12, 80-952 Gdańsk, Poland

Received: October 12, 2007; In Final Form: November 30, 2007

The hydration of formamide (F), *N*-methylformamide (NMF), *N*,*N*-dimethylformamide (DMF), acetamide (A), *N*-methylacetamide (NMA), and *N*,*N*-dimethylacetamide (DMA) has been studied in aqueous solutions by means of FTIR spectra of HDO isotopically diluted in H_2O. The difference spectra procedure has been applied to remove the contribution of bulk water and thus to separate the spectra of solute-affected HDO. To facilitate the interpretation of obtained spectral results, DFT calculations of aqueous amide clusters were performed. Molecular dynamics (MD) simulation for the cis and trans forms of NMA was also carried out for the SPC model of water. Infrared spectra reveal that only two to three water molecules from the surrounding of the amides are statistically affected, from among ca. 30 molecules present in the first hydration sphere. The structural−energetic characteristic of these solute-affected water molecules differs only slightly from that in the bulk and corresponds to the clathrate-like hydrogen-bonded cage typical for hydrophobic hydration, with the possible exception of F. MD simulations confirm such organization of water molecules in the first hydration sphere of NMA and indicate a practical lack of orientation and energetic effects beyond this sphere. The geometry of hydrogen-bonded water molecules in the first hydration sphere is very similar to that in the bulk phase, but MD simulations have affirmed subtle differences recognized by the spectral method and enabled their understanding. The spectral data and simulations results are highly compatible. In the case of F, NMF, and A, there is a visible spectral effect of water interactions with N−H groups, which have destabilizing influence on the amides hydration shell. There is no spectral sign of such interaction for NMA as the solute. The energetic stability of water H-bonds in the amide hydration sphere and in the bulk fulfills the order: NMA > DMA > A > NMF > bulk > DMF > F. Microscopic parameters of water organization around the amides obtained from the spectra, which have been used in the hydration model based on volumetric data, confirm the more hydrophobic character of the first three amides in this sequence. The increased stability of the hydration sphere of NMA relative to DMA and of NMF relative to DMF seems to have its origin in different geometries, and so the stability, of water cages containing the amides.

Introduction

The general opinion reigns that the specific organization of the hydrogen-bond network of water in hydrophobic and hydrophilic areas of biopolymers in their native state determines their tertiary and quaternary structure, and thus their life functions. However, the investigations of specific properties of water in biological systems encounter difficulties. First, because of the high degree of complication of such systems and, second, because of difficulty in isolating the contribution of water molecules, which are affected by a solute.

Amides provide a simplified example of the peptide linkage and represent an excellent model system for the study of both hydrophobic and hydrophilic interactions. The peptide group is a basic repeating unit of polypeptides and proteins. Molecular interactions of this functional group play an essential role in determining the structures and properties of biological systems. Therefore, understanding how these groups can interact with each other and with the surrounding solvent molecules can give information explaining the formation of the native structure of proteins.

For the above-mentioned reasons, we attempted to provide subtle molecular characteristics of the hydration layer of simple amides that differ in the number and vicinity of methyl groups: formamide (F), *N*-methylformamide (NMF), *N*,*N*-dimethylformamide (DMF), acetamide (A), *N*-methylacetamide (NMA), and *N*,*N*-dimethylacetamide (DMA).

Amides and their water clusters have been until now extensively studied experimentally by means of IR spectroscopy,[1−7] NMR spectroscopy,[2,8−11] microwave spectroscopy,[12−15] X-ray diffraction,[16−18] neutron diffraction,[19] electron diffraction,[20,21] and dielectric relaxation[22,23] and theoretically by ab initio calculations with various basis sets,[1,2,7,13,17,24−56] and by simulations with both Monte Carlo[34,56−63] and molecular dynamics (MD) methods.[9,48,56,64−75] Several studies were focused on the trans−cis equilibrium around the C−N bond of NMF and NMA molecules:[2,7,13,15,17,43,53,56] for amides, where cis and trans refer to the orientation of the C═O and N−H bonds with respect to the C−N bond. The general opinion prevails that the trans form is more stable in the gas phase as well as in aqueous solution.

We have used FTIR spectroscopy and the technique of isotopic dilution of HDO in H_2O, which is free from most experimental and interpretative problems connected with H_2O spectra.[76−78] The decoupled OD vibrations of HDO appear to be the most sensitive and ideally suited probe of solute hydration. To extract information about the interactions within

* Corresponding author. E-mail: stangret@chem.pg.gda.pl.

10.1021/jp7099509 CCC: $40.75
Published on Web 02/05/2008

the hydration sphere, the contribution of bulk water should be eliminated from the spectrum of the solution to obtain the solute-affected water spectrum. The corresponding method of spectra analysis originates from the works of Eriksson et al.[79,80] The quantitative version of this method, used in this work, was developed in our laboratory.[81,82] The solute-affected water spectra allow registering even short-lived species ($\sim 10^{-14}$ s) formed by water molecules influenced by a solute, which can be described in terms of their energetic state basing on the Badger−Bauer rule.[83] It states that the position of the water stretching vibration band changes proportionally with the energy of the hydrogen bond (lower wavenumbers correspond to stronger H-bonds). The considered spectra provide also basic structural characteristic of the solute-affected water, as the OD band position can be correlated with interatomic oxygen−oxygen distance.[84] The obtained experimental results are confronted with ab initio calculated structures of aqueous clusters of the solutes in the gas phase and using the polarized continuum model (PCM), as well as with simulations by the MD method.

Experimental Section

Chemicals and Solutions. Formamide (99.5+%, A.C.S. reagent, Aldrich), *N*-methylformamide (99%, Fluka), *N*,*N*-dimethylformamide (99.8%, Aldrich), acetamide (99%, Fluka), *N*-methylacetamide (99+% GC, Aldrich), and *N*,*N*-dimethylacetamide (99%, Aldrich) were used as supplied. D_2O (99.84% deuterium) was produced by the Institute of Nuclear Investigation of Poland. H_2O used for measurements was redistilled.

Stock solutions with H_2O were prepared for each solution series of spectra. Sample solutions for the HDO spectra were made by adding 4% (by weight) of D_2O relative to H_2O ($H_2O + D_2O = 2HDO$, $K \approx 4$) and the reference solutions (without D_2O) by adding the same molar amounts of H_2O. All solutions have been prepared by weight, and their densities were measured using an Anton Paar DMA 5000 densitometer at 25.000 ± 0.001 °C.

IR Measurements. FTIR spectra were recorded on Nicolet 8700 spectrometer (Thermo Electron Co.). For each spectrum 128 scans were made with a selected resolution of 4 cm^{-1}. A cell with CaF_2 windows was employed. The path length was 0.0289 mm, as determined interferometrically. The temperature was kept at 25.0 ± 0.1 °C by circulating thermostated water through the mounting plates of the cell. The temperature was monitored by a thermocouple inside the cell.

HDO spectra have been measured for solution molalities (m) in the range between 0 and 1 mol·kg^{-1}, in ca. 0.2 mol·kg^{-1} steps. The approximation of molar absorption coefficient values vs molality at each wavenumber measured has been verified to be the most justified by using linear regression for all the solutes studied ($R^2 > 0.9999$).

Analysis of Spectral Data. The method of analysis of the spectral data toward extraction of the solute-affected water spectrum has been described in ref 81. It assumes that water in solution may be divided into additive contributions of bulk (b) and solute-affected water (a). The spectrum of solute-affected water in molar absorptivity scale (ϵ_a) is defined for each wavenumber as

$$\epsilon_a = \frac{1}{NMm}(\epsilon - \epsilon_b) + \epsilon_b \qquad (1)$$

where ϵ is the spectrum of water in solution at molality m (mol kg^{-1}), ϵ_b is the spectrum of bulk water identical to the spectrum of pure water, N is a parameter (called "affected number") that denotes the number of moles of water affected by 1 mol of a solute, and M is the mean (4% D_2O in H_2O in the case of HDO spectra) molecular weight of water (kg mol^{-1}). Equation 1 makes the basis for extraction of solute-affected water spectrum at molality m. When $m \rightarrow 0$, eq 1 reduces to

$$\epsilon_a = \frac{1}{NM}\left(\frac{\partial \epsilon}{\partial m}\right)_{m=0} + \epsilon_b \qquad (2)$$

Passing the procedure of approximation of ϵ vs m, eq 2 enables the determination of solute-affected water spectrum extrapolated to infinite dilution when the affected number (N) is known. The proper value of N can be found on the basis of the spectra deconvolution procedure, according to the published algorithm.[82] The solute-affected spectrum and the N value are obtained simultaneously.

The spectra were handled and analyzed using the commercial PC programs GRAMS/32 (Galactic Industries Corp., Salem, MA) and RAZOR (Spectrum Square Associates, Ithaca, NY) run under GRAMS/32.

Ab Initio Computational Details. Ab initio molecular calculations were performed using the GAUSIAN 03 program package.[85] The nonhydrated and the hydrated structures of amides have been optimized in the framework of density functional theory (DFT) with B3LYP hybrid functional[86] using the 6-311++G(d,p) basis set.[87] The polarized continuum model (PCM) of self-consistent reaction field theory (SCRF) was used in some cases to study the systems in the liquid phase.

Details of Simulation Procedure. Molecular dynamics simulations were carried out at 298 K at constant pressure. Periodic boundary conditions were used. The system contained the NMA molecule, in the cis or the trans form, immersed within 506 water molecules in a cubic box. The program GROMOS96 was used for the simulations.[88] The SPC model was used for water molecules: the Lennard-Jones parameters $\epsilon_0 = 0.65017$ kJ mol^{-1}, $\sigma_O = 0.31656$ nm; the partial charges on atoms $q_O = -0.82e$, $q_H = +0.41e$; the bond length $r_{O-H} = 0.0100$ nm; the angle between bonds $\Theta_{HOH} = 109.47°$. OPLS parameters for the cis and trans forms of NMA molecule were taken from ref 56. Simulation was carried up in 0.002 ps steps, trajectories have been stored after two iterations (0.004 ps), and the total simulation time was 4 ns.

To analyze simulation results, each water molecule was arranged within its "own" coordinate system. As the Cartesian coordinates x, y, z we use main axes of the inertia tensor of the water molecule, ordered in such manner that $I_x < I_y < I_z$. The center of mass of the water molecule coincides with the origin (Figure 1a).

The definition of hydrogen bonding was used according to ref 89. The geometry of H-bonds between water molecules, which fulfill the definition of hydrogen bonding used, is characterized by the intermolecular oxygen−oxygen distance R_{OO} and by the angle β, defined in Figure 1b. We demanded, moreover, that the total interaction energy between two H-bonded molecules was negative; it is roughly equivalent to demanding that the force acting between these molecules is attractive. Their total interaction energy was calculated as the sum of both Lennard-Jones and electrostatic terms and its absolute value, averaged over all H-bonded molecules, was assumed as the mean H-bond energy of the system.

The distance between water and the amide molecule corresponds to the distance between the centers of mass of both molecules. To characterize the spatial orientation of water molecules relative to the amide molecule, radius vector (r) from the mass center of the amide molecule to the mass center of

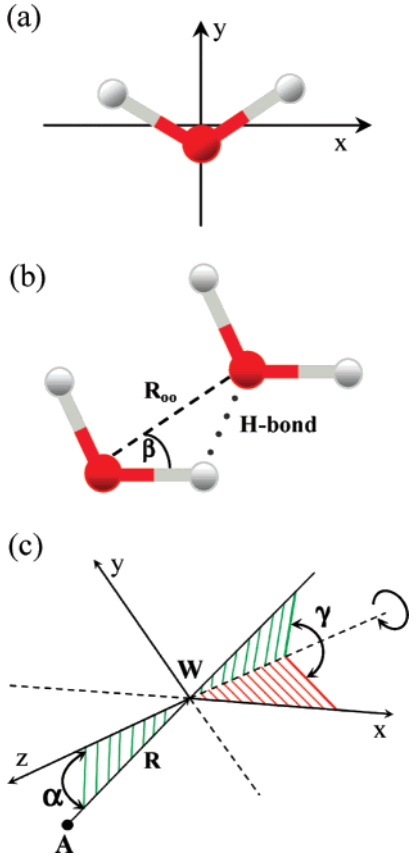

Figure 1. Definitions of the geometric parameters used in MD simulations: (a) orientation of principal axes of the water molecule, (b) oxygen−oxygen distance, R_{OO}, and angle β characterizing H-bonds of water molecules, and (c) the spatial orientation of the water molecule with respect to the amide molecule.

the water molecule was used, as well as two angles. The angle α denotes the angle between the radius vector *r* and the OZ axis of the "own" water molecule coordinate system. When α is not equal to zero, the two vectors *r* and OZ determine a plane. The angle γ denotes the angle between two planes: the plane determined by vector *r* and OZ axis and the plane determined by OX and OZ axes of the "own" water molecule coordinate system (Figure 1c).

Results and Discussion

Affected HDO Spectra. In Figure 2 the derivatives $(\partial\epsilon/\partial m)_{m=0}$ for the studied amides have been shown together with the bulk HDO spectrum, for better comparison. They have been used to determine solute-affected HDO spectra according to eq 2 and the procedure of band shape analysis previously described in detail.[82] The following adjusted *N* values were found: 1.7 (F), 2.8 (NMF), 2.8 (DMF), 2.0 (A), 2.9 (NMA), 2.9 (DMA). Amide-affected water spectra have been shown in Figures 3 and 4, together with the minimal number of analytical symmetrical components bands, of the general shape described as the product of Gaussian and Lorentzian peak functions, which adequately approximate the band shape of solute-affected HDO spectra. The adjusted spectra do not include the bulk HDO spectrum, but analytical component bonds do not necessarily possess physical significance. This is because of the proved asymmetry of "normal" HDO bands, connected with the known effect of increasing integral intensity with the band shift toward lower wavenumbers.[90,91] As a result, the simple HDO band could be a superposition of two or more symmetrical analytical component bands.

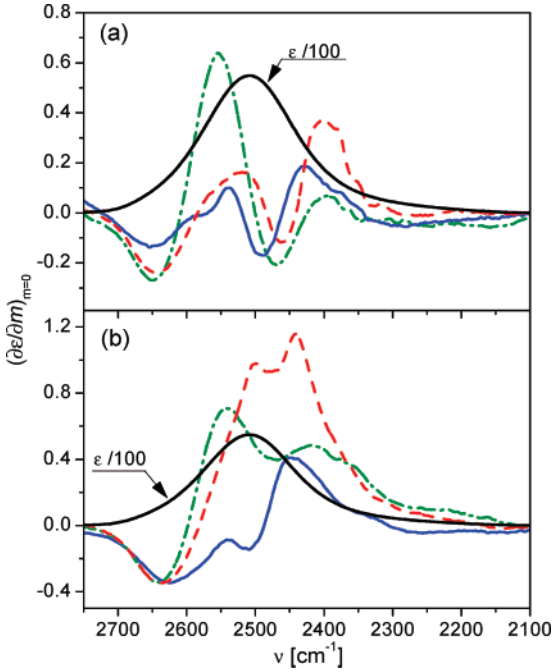

Figure 2. Derivatives $(\partial\epsilon/\partial m)_{m=0}$ for HDO spectra of aqueous solutions of (a) F (solid line), NMF (dashed line), DMF (dashed−dotted line), and (b) A (solid), NMA (dashed), DMA (dashed−dotted). The bulk HDO spectrum (black solid line) has been shown for comparison purposes (in molar absorptivity scale divided by 100).

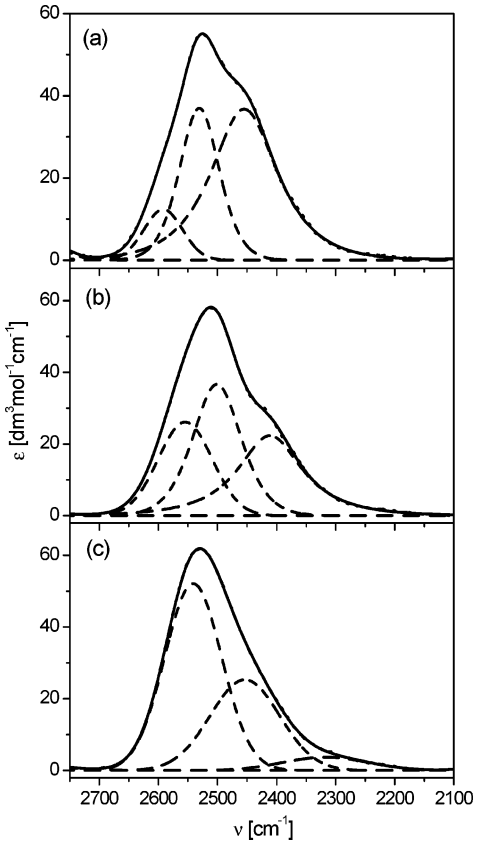

Figure 3. Decomposition of HDO spectra, affected by (a) F, (b) NMF, and (c) DMF, into analytical component bands. Solid line, original affected spectrum; dashed lines, component bands; dotted line, sum of the component bands.

Band shapes for DMF- and DMA-affected water shown in Figures 3c and 4c, respectively, correspond solely to OD stretching vibrations of HDO. On the other hand, affected spectra

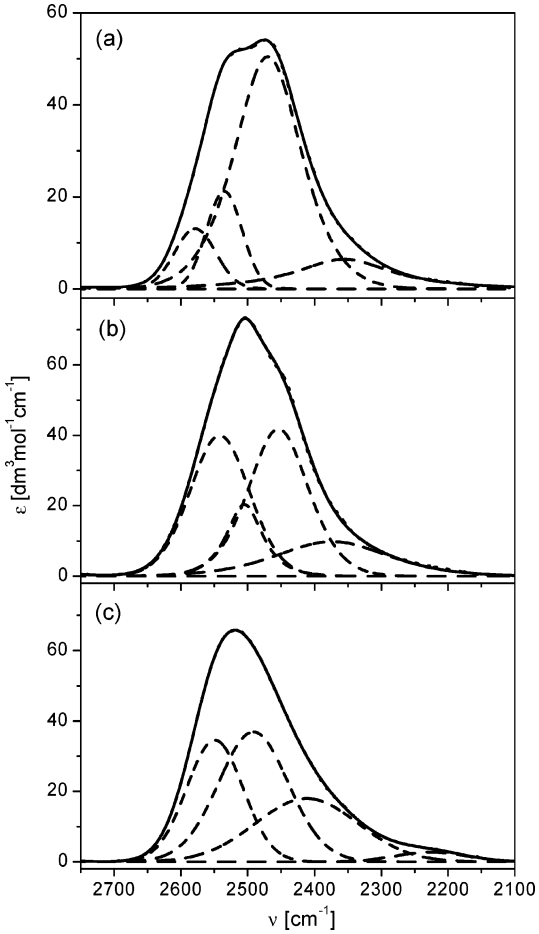

Figure 4. Decomposition of HDO spectra affected by (a) A, (b) NMA, and (c) DMA, into analytical component bands. Solid line: original affected spectrum; dashed lines: component bands; dotted line, sum of the component bands.

for F and NMF (Figure 3a,b), as well as for A and NMA (Figure 4a,b) included also ND stretching vibration band as a result of isotopic substitution. They appear as shoulders on the low-wavenumbers slope of the corresponding amide-affected spectra. To isolate ν(ND) bands, the band shape of DMF-affected water spectrum has been used to re-deconvolute affected HDO spectra of F and NMF from Figure 3a,b, and the band shape of DMA-affected water spectrum has been used to re-deconvolute affected spectra HDO of A and NMA from Figure 4a,b. In the procedure of this re-deconvolution, the band shape of DMF- and DMA-affected water was allowed to change the position, the height, and even the width at half-height but not the shape described by the symmetry factor used in the algorithm of band fitting. The adequate approximation of the spectra of F- and NMF-affected HDO, as well as of A and NMA ones, required additional analytical band components, which we believe to possess physical significance. They have been shown in Figures 5 and 6.

The F-affected HDO spectrum (Figure 5a) does not include the composite band with the position in maximum at 2440 cm^{-1} and gravity center at 2424 cm^{-1}, because it is attributed to the stretching vibration of isotopically substituted N−D formamide groups. The shape of the composite band is strongly asymmetric, which is the symptom of hydrogen bonding with surrounding water molecules. The HDO molecules interacting with this amino group build a high-wavenumber component band at ca. 2600 cm^{-1}. This band is also visualized on the corresponding derivative, as a shoulder in Figure 2a. The appearance of the

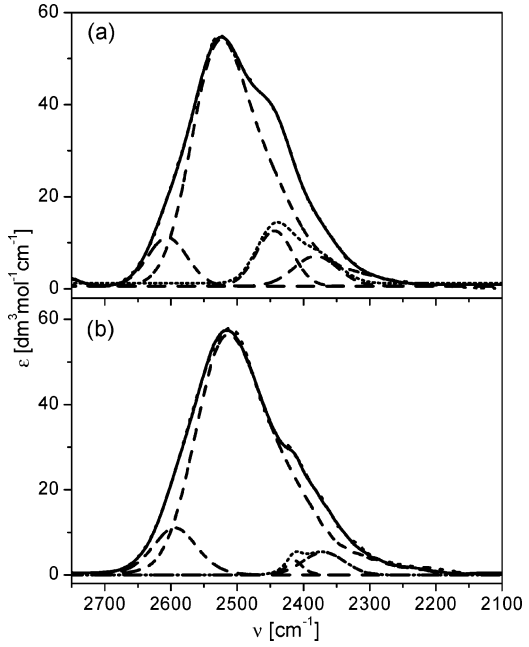

Figure 5. Decomposition of HDO spectra affected by (a) F and (b) NMF (dotted line), as to isolate N−D stretching vibration bands; see the text.

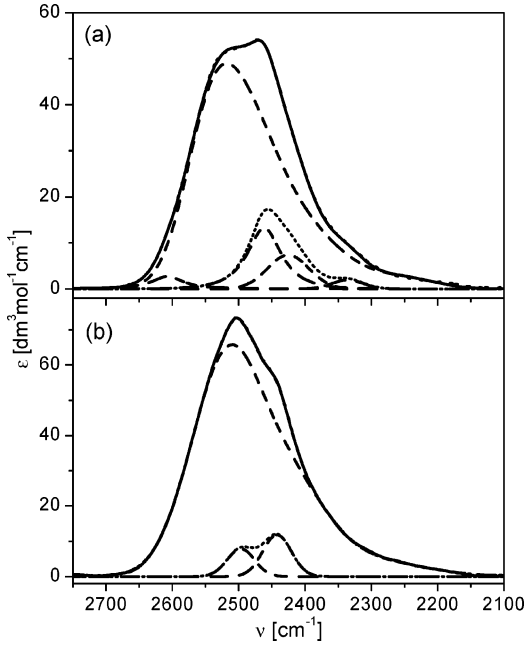

Figure 6. Decomposition of HDO spectra affected by (a) A and (b) NMA (dotted line), as to isolate N−D stretching vibration bands; see the text.

discussed band component means that F-affected HDO forms more weak H-bonds than HDO affected by DMF (which has been used as the model for the peak-fitting procedure). These weakly H-bonded water molecules interact with hydrogen atoms of amino groups of formamide. The situation is alike for the A-affected HDO spectrum, shown in Figure 6a. The ν(ND) band has it maximum at 2455 cm^{-1} and the position of the gravity center at 2443 cm^{-1}. Thus, the asymmetry is less pronounced than for the F-affected HDO. It can be the sign that amine groups of A are less involved in H-bonding with surrounding water molecules. The accompanying high-wavenumber component band at ca. 2600 cm^{-1} is also less pronounced than the corresponding one for F. It means that water molecules surrounding amino groups of A form only to a small extent

TABLE 1: Experimental and Theoretical Values of ν(ND) Band Position

		$\nu_{ND}{}^a$	$\nu_{ND}{}^b$
NMF	trans	2415	2455
	cis	2370	2415
NMA	trans	2497	2485
	cis	2442	2440

[a] Experimental values of ν(ND) band position (cm^{-1}). [b] Calculated (DFT method, PCM model) values of ν(ND) band position (cm^{-1}).

TABLE 2: Calculated Energy for NMF and NMA Molecules in the Trans and Cis Conformations for the Gas Phase and for the Continuum Aqueous Phase (PCM Model)

		gas phase		PCM	
		E^a	ΔE^b	E^a	ΔE^b
NMF	trans	−209.198 855	−7.5	−209.216 876	−4
	cis	−209.195 995		−209.215 393	
NMA	trans	−248.504 389	−12.5	−248.520 160	−6.2
	cis	−248.499 649		−248.517812	

[a] Calculated energy (hartree). [b] Energy difference between the trans and cis form ($kJ \cdot mol^{-1}$).

weaker H-bonds than from DMA surroundings (used as the model for the peak-fitting procedure), in the opposition to the F case.

A somewhat different case concerns the NMF-affected HDO spectrum (Figure 5b) and the NMA-affected one (Figure 6b), because these amides occur in solution as the trans and cis isomers. The ν(ND) bands in both cases are composed of two components, and every time the trans forms vibrates at higher wavenumbers. The corresponding band positions are included in Table 1 along with data calculated by the DFT method within the PCM model. As can be seen, the experimental and calculated data are generally in a good agreement. The band positions for NMA are especially consistent, whereas for NMF the calculated positions are distinctly higher. This is a meaningful result, because calculations do not take explicitly into account the H-bonds of water molecules with hydrogen atom of amino groups and the effect of H-bonding consists of ν(ND) band shifting toward lower wavenumbers. This should signify that, in the case of NMF, the hydrogen atom of the amino group forms a hydrogen bond with surrounding water molecules and that there is no such interaction in the case of NMA. This conclusion is strongly supported by the presence of a high-wavenumber component band at ca. 2600 cm^{-1} (Figure 5b), which arises from HDO molecules H-bonded to proton of NMF amino group. There is no such band in the case of NMA (Figure 6b).

Results of calculated energy for NMF and NMA molecules in the trans and cis conformations have been shown in Table 2 for the gas phase and for the continuum aqueous phase (PCM model). The values obtained are compatible with previously reported data.[15,17] It is evident that the trans isomer is more stable for both amides, but the energy difference decreases in the solvent. This can be compared with the spectral data, as the intensity of the ν(ND) bands should be a measure of the contribution of both forms in aqueous solution. The spectra suggest that both isomers of NMA may exist in water in comparable amounts and an even larger population of cis form is expected for NMF. The last statement could be justified by the already stated fact that NMF forms H-bond with water molecules via the H atom of the amino group and that the cis form has more acidic character, as indicated by lower force-constant for the N−D vibration in *cis*-NMA (Table 1) and the larger positive charge on the amino hydrogen atom for the *cis*-NMA used in the parametrization for molecular dynamics simulations.

TABLE 3: Solute-Affected and Bulk OD Band Positions of HDO and the Respective Interatomic Oxygen−Oxygen Distances

solute	N^a	$\nu^o{}_{OD}{}^b$	$\nu^c{}_{OD}{}^c$	fwhh[d]	I^e	$R_{OO}{}^{o\,f}$	$R_{OO}{}^{c\,g}$
bulk water		2509	2505	162	10096	2.828	2.843
F	1.7	2524	2515	139	8362	2.853	2.857
NMF	2.8	2517	2503	155	9639	2.838	2.841
DMF	2.8	2528	2511	155	10595	2.851	2.849
A	2.0	2519	2497	156	8698	2.838	2.835
NMA	2.9	2509	2492	167	11978	2.830	2.827
DMA	2.9	2519	2497	166	12312	2.835	2.833

[a] Affected number. [b] Band position at maximum (cm^{-1}). [c] Band position at gravity center (cm^{-1}). [d] Full-width at half-height (cm^{-1}). [e] Integrated intensity ($dm^3 \cdot mol^{-1} \cdot cm^{-1}$). [f] The most probable O···O distance (Å). [g] Mean O···O distance (Å).

Amide-affected HDO spectra for F, NMF, A, and NMA can be obtained by deleting the ν(ND) component bands from the spectra in Figures 5 and 6. Their shapes, together with the shapes of DMF- and DMA-affected HDO spectra from Figures 3c and 4c, have been compared and later analyzed by transforming spectral band shapes to the oxygen−oxygen distance distribution function $P(R_{OO})$ of water molecules, calculated according to the previously published procedure,[80,82] tested extensively, and found valid for aqueous solutions (see for instance refs 82 and 84 and references therein). The algorithm used is based on the ν_{OD} vs R_{OO} correlation curve constructed from experimental data on solid hydrates.[92] This relation intrinsically includes only nearest neighbor interactions in water and asymptotically reaches 2727 cm^{-1} (ν_{OD} value in the gas phase) as R_{OO} tends to infinity. This asymptotic behavior is then shown also by $P(R_{OO})$ curves, which fall asymptotically to zero as R_{OO} increases.

Band parameters for all studied amide-affected HDO bands, together with the bulk HDO band, are shown in Table 3 along with the respective R_{OO} data. In this table we have distinguished two values of band position, in the maximum (ν^o) and in the gravity center (ν^g), as a measure (by application of the Badger−Bauer rule) of the most probable and the mean energy of water H-bonds. Accordingly, the most probable ($R_{OO}{}^o$) and the mean ($R_{OO}{}^g$) oxygen−oxygen intermolecular distance have been discriminated.

Oxygen−oxygen distance distribution functions of amide-affected water and bulk water are shown in Figure 7. As recently suggested,[84] this is the most rational way, arising from infrared data, to compare and characterize the structural−energetic state of hydrating water. As can be seen, all these functions only slightly differ from each other and are very similar to the function for pure water. To visualize the difference in intermolecular distances, the result of subtraction of the distribution function for amide−affected water and for bulk water, $\Delta P(R_{OO})$, is shown in Figure 8 for each studied amide.

It is evident from Figure 8 that acetamide derivatives organize surrounding water molecules stronger than formamide derivatives. Both series of amides decrease the population of very weak H-bonds, as evidenced by negative $\Delta P(R_{OO})$ values above ca. 2.95−3.0 Å, which is the typical effect for hydrophobic hydration,[82,84,93] but for acetamide derivatives this effect is very pronounced. All the solutes increase the population ($\Delta P(R_{OO}) > 0$) of slightly longer oxygen−oxygen distances ($R_{OO} = 2.85$−2.95 Å) than the most probable distance for bulk water (2.83 Å, Table 3), which is also typical for hydrophobic solutes. Excluding formamide, all the remaining amides increase the population of strong H-bonding of surrounding water molecules.

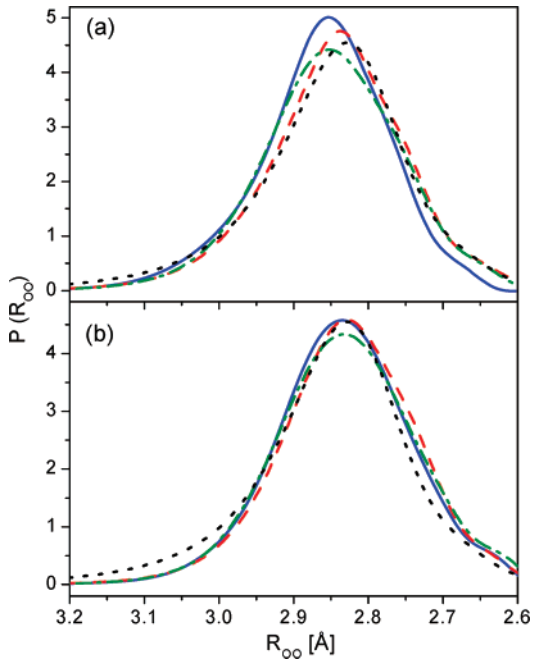

Figure 7. Interatomic oxygen−oxygen distance distribution derived from the HDO spectra affected by (a) F (blue), NMF (red), and DMF (green) and (b) A (blue), NMA (red), and DMA (green), along with the bulk HDO (black) distance distribution curve.

Their structure is characterized by the oxygen−oxygen distance of ca. 2.74 Å, which correspond roughly to the distance typical for water in the ice phase (2.76 Å). We want to stress that this is not the effect of water molecules H-bonded to an electrophilic center of a solute, as the same effect is also observed for tetrabutylammonium cation (Figure 8c), studied previously in our laboratory as a model for hydrophobic hydration.[82]

Another interesting conclusion results from Figure 8. Replacement of the first amino hydrogen atom by the methyl group distinctly increases the ability of an amide to function as a "structure-making" solute. This substitution results in decreasing the contribution of weak H-bonded water molecules (decreasing of long oxygen−oxygen distances) and increasing the "ice-like" water contribution (increasing of short "ice-like" oxygen−oxygen distances). More unexpected is the observation that substitution of the second hydrogen atom by a methyl group diminishes this effect. Thereby, NMA appears as the most water "structure-making" solute among the studied amides. From comparison of ν^g and $R_{OO}{}^g$ values for this solute and for bulk water (Table 3) it is clear that water affected by NMA forms on average stronger H-bonds and is more ordered than pure water. Simultaneously, because of the superstructure, NMA molecule seems to fulfill conditions as the best model, among the amides studied, for a basic repeating unit of polypeptides and proteins. For that reason, hydration of NMA has been additionally simulated by means of the molecular dynamics method.

More hydrophobic character of methyl-substituted amides has been additionally confirmed by correlations presented in Figure 9. They use the simple linear relationship between volumetric data of solution and the change of the oxygen−oxygen distance in water structure due to solute−solvent interactions ($\Delta R_{OO} = R_{OO}{}^s - R_{OO}{}^b$), as well as the N parameter, obtained from infrared spectra. The relationship corresponds to the hydration model recently proposed in the form[84]

$$(V_\Phi{}^o - V_{vdW})/NS_{SAS} = b\Delta R_{OO} + a \qquad (3)$$

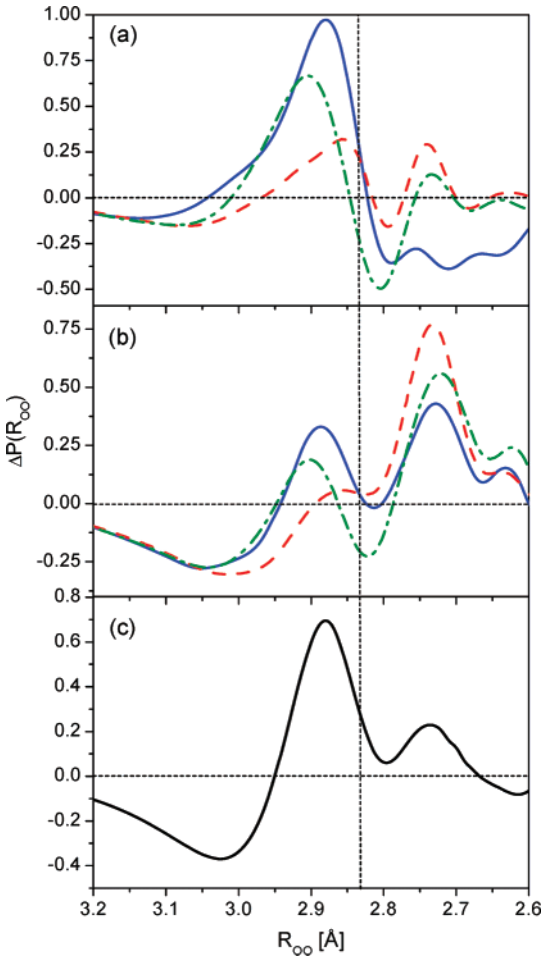

Figure 8. Difference between interatomic oxygen−oxygen distance distribution of affected water, $P(R_{OO}{}^a)$, and bulk water, $P(R_{OO}{}^b)$: (a) F (blue), NMF (red), and DMF (green); (b) A (blue), NMA (red), and DMA (green); and (c) tetrabutylammonium cation (black), studied previously in our laboratory (data taken from ref 82). The vertical line shown marks the average distance for bulk water.

where $V_\Phi{}^o$ and V_{vdW} denote, respectively, the limiting apparent molar volume and the van der Waals volume, S_{SAS} denotes the solvent-accessible surface of studied amides, parameter b is the correction constant of R_{OO} distance, and parameter a is the thickness of the empty volume space between the surface of a solute and the surface marked by average positions of solvent molecules in the first hydration layer. The solute parameters, V_{vdW} and S_{SAS}, have been calculated as previously reported.[84] All the respective data used for correlations are included in Table 4.

Both the relationship for the most probable oxygen−oxygen distance (Figure 9a), as well as for the mean distance (Figure 9b), show two distinct correlations, for the formamide and for the acetamide derivatives. In each case, the parameter a is bigger for the A, NMA, and DMA group (0.07 Å for the $\Delta R_{OO}{}^o$ relationship and 0.1 Å for the $\Delta R_{OO}{}^c$ relationship) than for the F, NMF, and DMF group (0.05 Å for the $\Delta R_{OO}{}^o$ relationship and 0.07 Å for the $\Delta R_{OO}{}^c$ relationship). The obtained result is consistent with the simplified hydration image of the A-type solute, where surrounding water molecules form H-bonds mainly between each other, forming a clathrate-type network. Water molecules from the hydration sphere of the second type of amide more often form H-bonds with the solute that is more electrophilic in character. Such view is also supported by DFT calculations.

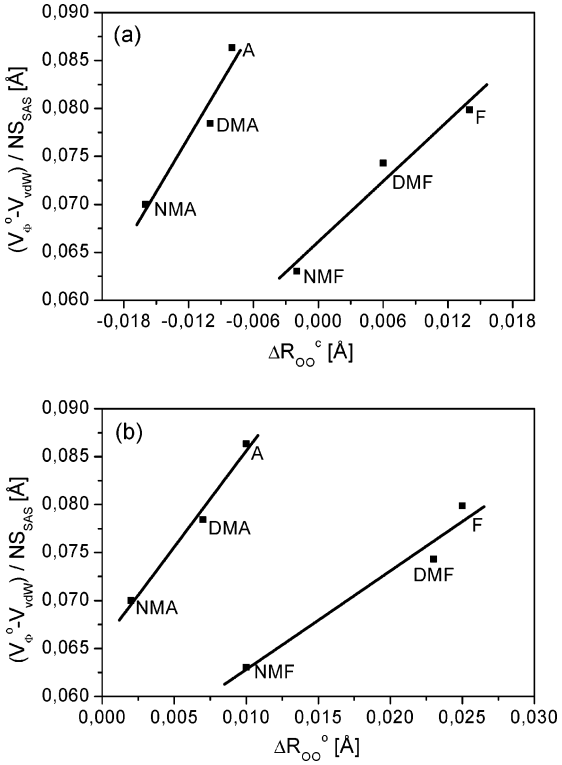

Figure 9. Correlation between the limiting apparent molar volume (V_Φ°), van der Waals volume (V_{vdW}), solvent accessible surface (S_{SAS}), and solute-affected number of solvent molecules (N) and the change of oxygen−oxygen distance of affected and bulk water molecules for (a) the mean distance (ΔR_{OO}^c) and (b) the most probable distance (ΔR_{OO}°). Data taken for correlations are included in Tables 3 and 4.

TABLE 4: Volumetric Data and Calculated Molecular Parameters for Studied Amides

solute	V_Φ° [a]	V_{vdW} [b]	V_{vdW} [c]	S_{SAS} [d]
F	38.5	40.67	24.50	103.12
NMF	56.8	58.22[e]	35.06[e]	123.06[e]
		58.26[f]	35.09[f]	123.76[f]
DMF	74.5	75.40	45.41	139.81
A	55.8	57.36	34.55	123.09
NMA	74.0	74.86[e]	45.09[e]	142.64[e]
		74.73[f]	45.01[f]	139.42[f]
DMA	90.5	91.71	55.24	155.00

[a] Limiting apparent molar volume ($cm^3 \cdot mol^{-1}$) (ref 94). [b] Calculated van der Waals volume (Å).[3] [c] Calculated van der Waals volume ($cm^3 \cdot mol^{-1}$). [d] Calculated solvent accessible surface ($10^4 \cdot m^2 \cdot mol^{-1}$). [e] Trans isomer. [f] Cis isomer.

Ab Initio Calculations. Results of DFT calculations of total and H-bond energies for the H-bonded clusters of amides and water are summarized in Table 5. The H-bonded centers of the amide have been defined in Figure 10. For NMF and NMA molecules only the trans form has been considered as more unequivocal in interpretation. Hydrogen-bonded energy has been calculated as the difference between the energy of a cluster and the sum of the energies of separated molecules, as in ref 48. Additionally, the reciprocal influence of H-bonds has been characterized by calculating the energy difference between the multihydrated amide cluster and the sum of the respective monohydrates of the amide. The energy of the H-bond of water dimer has been also included in Table 5 for comparison purposes.

It is apparent from Table 5 that water molecule interacts distinctly more strongly with the carbonyl oxygen atom than with the amine group proton. The interaction with carbonyl group generally follows the order of donor abilities of studied amides. The H-bond energy calculated for the water dimer (14.76 $kJ \cdot mol^{-1}$) appears to be lower than for any other water interaction with the amide molecule. However, it is incorrect to draw a general opinion that in aqueous solution water interacts more strongly with the amide than with other water molecules, because of water H-bond cooperativity. This effect is relatively well recognized; Gutmann's donor number (DN) for water changes from DN = 18 for gas phase to DN = 26.7 for liquid water.[95] For comparison, DN(DMF) = 26.6 and DN(DMA) = 27.8.[96] Thus, taking into account the calculated energy of water H-bonded to DMF and DMA carbonyl group, respectively 21.48 and 30.59 $kJ \cdot mol^{-1}$ on average, the H-bond energy of water in aqueous solution can be estimated to 22.2 $kJ \cdot mol^{-1}$ (within the scale determined by the method of calculation). This value should be compared with the data from Table 5: the energy of water H-bonded to the a sites of F and A (Figure 10) is not meaningful in that respect, because water molecule interacts simultaneously with carbonyl oxygen and amine proton of the amide.

TABLE 5: Total and Hydrogen-Bond Energies for the Hydrogen-Bonded Clusters of Amides and Water Calculated at the B3LYP/6−311++G(d,p) Level in the Gas Phase

		E^a	E_{H-bond} [b]	ΔE^c
	H_2O	−76.437 243		
	dimer H_2O	−152.880 110	14.76	
	F	−169.909 617		
a	F + H_2O	−246.357 647	28.322	
b	F + H_2O	−246.354 178	19.214	
c	F + H_2O	−246.353 236	16.740	
a + b	F + $2H_2O$	−322.801 954	46.869	−0.667
a + c	F + $2H_2O$	−322.801 720	46.254	+1.192
b + c	F + $2H_2O$	−322.799 243	39.751	+3.797
a + b + c	F + $3H_2O$	−399.247 083	67.574	+3.298
	A	−209.215 623		
a	A + H_2O	−285.664 334	30.110	
b	A + H_2O	−285.661 250	22.013	
c	A + H_2O	−285.658 916	15.885	
a + b	A + $2H_2O$	−362.109 480	50.859	−1.264
a + c	A + $2H_2O$	−362.107 949	46.840	+0.845
b + c	A + $2H_2O$	−362.105 722	40.993	+3.095
a + b + c	A + $3H_2O$	−438.554 023	70.026	+2.018
	trans-NMF	−209.198 855		
a	NMF + H_2O	−285.644 047	20.870	
b	NMF + H_2O	−285.643 954	20.626	
c	NMF + H_2O	−285.642 548	16.935	
a + b	NMF + $2H_2O$	−362.088 051	38.622	−2.874
a + c	NMF + $2H_2O$	−362.088 804	40.599	+2.794
b + c	NMF + $2H_2O$	−362.088 804	40.599	+3.038
a + b + c	NMF + $3H_2O$	−438.533 693	60.674	+2.243
	trans-NMA	−248.504 389		
a	NMA + H_2O	−324.950 580	23.493	
b	NMA + H_2O	−324.950 924	24.397	
c	NMA + H_2O	−324.947 279	14.826	
a + b	NMA + $2H_2O$	−401.395 320	43.177	−4.713
a + c	NMA + $2H_2O$	−401.394 653	41.426	+3.107
b + c	NMA + $2H_2O$	−401.395 066	42.510	+3.287
a + b + c	NMA + $3H_2O$	−477.840 278	63.433	+0.717
	DMF	−248.488 510		
a	DMF + H_2O	−324.933 780	21.075	
b	DMF + H_2O	−324.934 087	21.881	
a + b	DMF + $2H_2O$	−401.378 122	39.714	−3.242
	DMA	−287.786 188		
a	DMA + H_2O	−364.234 581	29.275	
b	DMA + H_2O	−364.235 579	31.895	
a + b	DMA + $2H_2O$	−440.679 539	49.531	−11.639

[a] Total energy (hartree). [b] Hydrogen-bond energy defined as the difference between the energy of a cluster and the sum of the energies of separated molecules ($kJ \cdot mol^{-1}$). [c] Hydrogen-bond energy differences between polyhydrated clusters and sum of hydrogen-bond energy of monohydrated amides ($kJ \cdot mol^{-1}$).

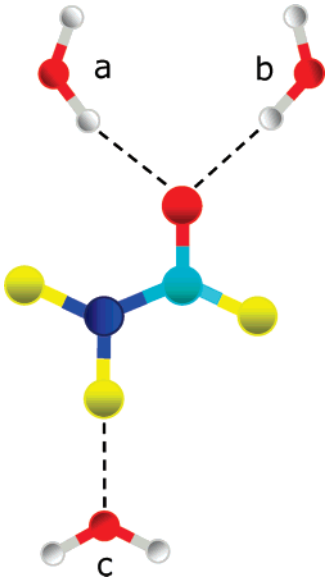

Figure 10. Structure of amide hydrogen bonded with three water molecules and the definition of the bonded centers related to hydrogen bonds; yellow balls denote H or CH_3, depending on the amide.

Interesting observations appear from the comparison of the reciprocal influence of water H-bonds with amides (ΔE values in Table 5). It is clear that the anticooperative effect for two water molecules H-bonded to carbonyl group takes place and also that cooperativity occurs for water molecules interacting simultaneously with oxygen and amine proton of the amide. An especially weak anticooperative effect and a strong cooperative effect are observed for F. It is caused by mainly the electrophilic character of F, which is ready to form the maximum number of H-bonds with water in aqueous solution. On the other hand, an especially strong anticooperative effect takes place for NMA and DMA, which does not favor formation of two simultaneous H-bonds between water molecules and the carbonyl group. Additionally, the water−NMA interaction via the amine proton is especially weak. All these circumstances imply that NMA and DMA avoid extensive interaction with water molecules, have the strongest hydrophobic character from the amides studied, and are the strongest "structure-making" solutes, as evidenced by infrared data.

Molecular Dynamics Results. Figure 11 summarizes results of MD simulations of hydration of *cis*- and *trans*-NMA. In Figure 11a, the computed radial distribution functions (rdfs) between the centers of mass of the amide and water molecules are presented. There are some differences between the cis- and trans-isomers resulting from the different shape of these molecules. From the course of rdfs, it seems reasonable to assume that the first hydration sphere of NMA molecule spreads in the range from 3.2 to 6.4 Å and the second one from 6.4 to 9.6 Å. Beyond this sphere, water molecules can be treated as the bulk phase. Water molecules within the consecutive spheres are characterized in Table 6. The first hydration sphere includes about 31 water molecules, which form on average somewhat stronger H-bonds than molecules from the outer sphere; around *trans*-NMA, H-bonds are subtly stronger. The average number of H-bonds per one water molecule in the first hydration sphere is lower than from the outer sphere.

It is possible to compare the effect of H-bond energy change for water molecules in the first hydration sphere of NMA relative to the bulk phase, when calculated per 1 mol of the solute, taking into account the MD simulation and spectral data. The ascription of the HDO band to a certain energetic state of water molecules

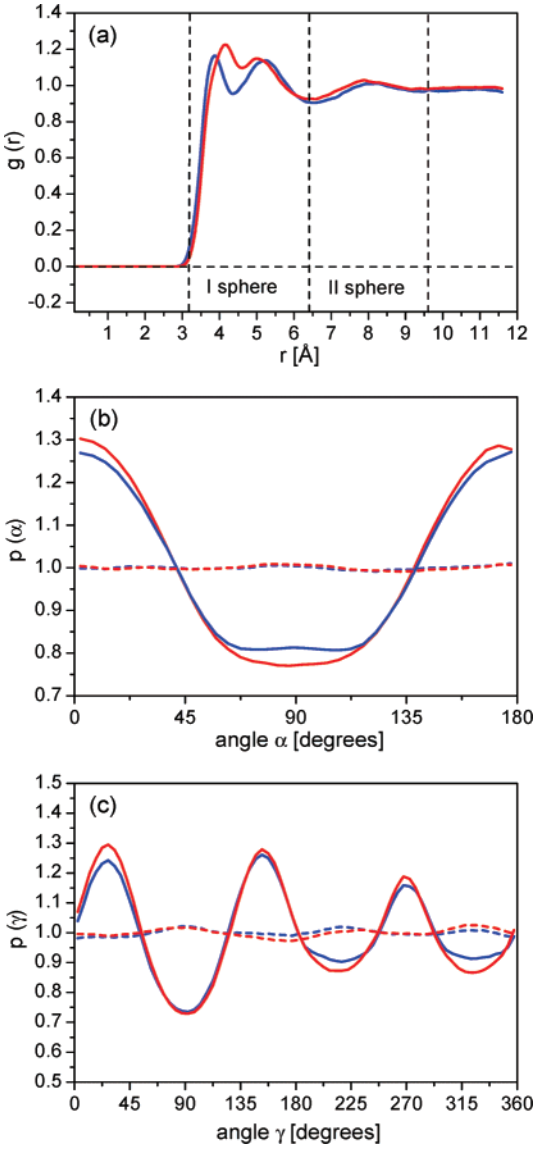

Figure 11. Results of MD simulations of aqueous solution of *cis*- (red) and *trans*-NMA (blue): (a) radial distribution function (between the centers of mass) of water molecules around the amide molecule, (b) distribution for α angle (see text) for the first (solid) and the second hydration sphere (dotted), (c) distribution for γ angle (see the text) for the first (solid) and the second hydration sphere (dotted).

TABLE 6: Data for Water Molecules Solvating the *cis*- and *trans*-NMA Obtained by Molecular Dynamics Simulations

NMA	distance range[a]	n^b	$n_{HB}{}^c$	$E_{HB}{}^d$	$R_{OO}{}^e$	β^f
trans	3.2−6.4	31.259	2.966	18.838	2.831	12.60
	6.4−9.6	82.645	3.035	18.389	2.832	12.69
	9.6−1.13	74.573	3.036	18.401	2.832	12.69
cis	3.2−6.4	31.313	2.963	18.525	2.831	12.64
	6.4−9.6	82.886	3.035	18.391	2.832	12.69
	9.6−1.13	74.382	3.036	18.393	2.832	12.69

[a] In Å. [b] Mean number of solvating molecules in the analyzed envelope. [c] Mean number of hydrogen bonds of solvating water molecules. [d] Mean energy of hydrogen bond between water molecules (kJ·mol^{-1}). [e] Mean O···O distance for water molecules (Å). [f] Mean value of angle β for hydrogen-bonded water molecules (deg).

in the hydration sphere may be achieved by transforming the OD band position, ν_{OD}, to the intermolecular interaction energy of water. The relationship linking this energy with ν_{OD} takes advantage of the Badger−Bauer rule[83] and the procedure described before.[97,98] Accordingly, taking the $\nu_{OD}{}^c$ values from

Table 3 for NMA (2492 cm^{-1}) and for bulk water (2505 cm^{-1}), the average change of the energy of hydrogen bonds for 1 mol of the affected water is equal to 2.57 kJ. Taking the number of water molecules affected by NMA ($N = 2.9$), the average H-bonds energy gain of water solvating 1 mol of NMA equals 7.5 kJ. To compare this value with the data obtained from MD simulation, the average number of water moles in the first hydration sphere per 1 mol of NMA (31.3 from Table 6) should be multiplied by the H-bond energy difference between water molecules in the first and the third hydration sphere (treated as bulk water) and also by the average number of water H-bonds. The first value, taken as the arithmetic mean for the *trans*- and *cis*-NMA, equals 0.285 kJ·mol^{-1}. The average number of water H-bonds in the first hydration sphere of the *trans*- and *cis*-NMA equals 2.965. To avoid counting twice the number of H-bonds in the considered system, this value should be divided by two. Assuming that water molecules form all H-bonds within the first hydration sphere, the average change of H-bond energy per 1 mol of NMA equals 13.2 kJ. More realistic estimation should take into account that statistically each water molecule from this sphere uses one H-bond to interact with molecules from the second hydration layer, and the rest are engaged in a clathrate-like network within the first sphere. This gives 8.8 kJ/mol of NMA and is close to the value obtained from the infrared data.

Figure 11b,c presents distributions for the angles α and γ (see section 2.5), which characterize the orientation of water molecules relative to the amide molecule. It is clear from the distribution of α that water molecules from the first hydration sphere are oriented on average parallel to the surface of the amide molecule, which strongly suggests clathrate-like type of hydration. This orientation is somewhat better specified for *cis*-NMA. From the distribution of γ one can deduce further details of that orientation. Angles larger than 180° correspond to an orientation where hydrogen atoms of the water molecule are slightly more "outside" from the amide surface than the oxygen atom. The opposite is true for γ smaller than 180°, where hydrogen atoms are closer to the amide molecule than to the oxygen atom. From the height of the maxima in Figure 11c, one can infer that the hydrated water cage has somewhat more hydrogen atoms oriented "inside" than "outside". This could be a result of the stronger orientation of water molecules via their interaction with the carbonyl oxygen atom than with the hydrogen atom of the NMA amine group. The effect is somewhat more marked for the *cis*-NMA. Water molecules from the second hydration sphere practically do not show preferable orientations relative to the solute. Differences between the hydration of the cis and trans form of NMA are small.

The geometry of water H-bonds is characterized by the distribution function of the angle β, shown in Figure 12a. The most probable angle differs only marginally for *trans*- and *cis*-NMA and within the following hydration spheres. It equals to ca. 10° and agrees very well with that obtained for liquid water on the basis of relaxation time measurements and ab initio calculations.[99] Figure 12b visualizes the subtle difference of angle β distribution between the first hydration sphere and the bulk phase. It is evident that water molecules from the first hydration sphere form more linear H-bonds, which should be one of the reasons for the slightly higher energy of water H-bonds in this sphere (Table 6).

The second parameter used to characterize the geometry of water H-bonds is oxygen−oxygen distance. To find the corresponding distance distribution function for water in the following hydration spheres of NMA molecule, the radial distribution

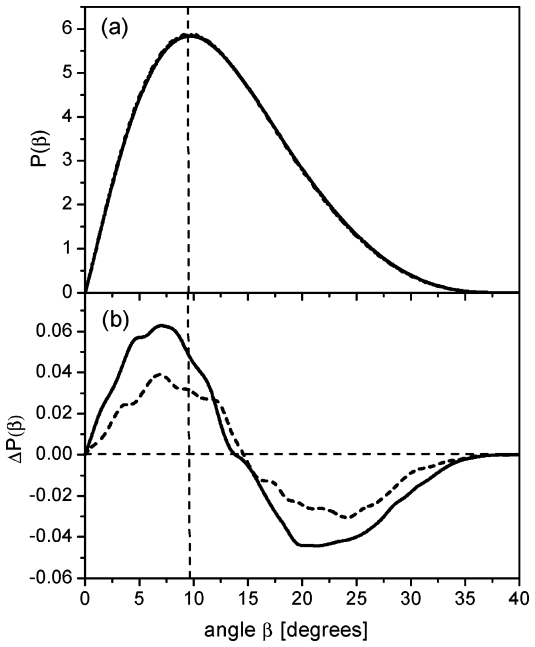

Figure 12. (a) Computed normalized distribution of β angle (see text) function for the *cis*- and *trans*-NMA in the first (solid) and second hydration sphere (dotted). (b) Difference between normalized distributions of β angle function for the *cis*- (dotted) and *trans*-NMA (solid) for the first and the third hydration sphere (treated as the bulk phase).

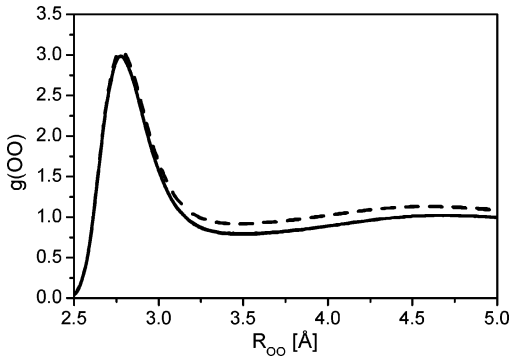

Figure 13. Computed radial distribution function for the oxygen−oxygen distance of water molecules in the first hydration sphere of the *cis*- and *trans*-NMA (solid) and also for the consecutive hydration spheres (dashed).

function for O···O distance has been preliminary calculated, g(OO), as shown in Figure 13. As can be seen, the most probable distance is practically the same for *trans*- and *cis*-NMA and also for the consecutive hydration spheres. Its course generally agrees with the previously reported data.[100,101] It appears that hydration spheres extend to the distance of ca. 3.5 Å, and this value is used for calculation of the O···O distance distribution function, $P(R_{OO})$, for the first, second, and third hydration sphere. Only those molecular pairs have been considered that obey the definition for the hydrogen bond accepted before. Results are shown in Figure 14a.

The O···O distance distribution function in Figure 14a for *trans*- and *cis*-NMA, as well as for three consecutive hydration spheres, coincides. The insert shown in this figure compares the distributions obtained from simulations and from infrared spectra of bulk water (Figure 7). The function derived from the spectra is narrower and has its maximum shifted toward longer distances. This maximum corresponds to the most probable distance. It is worth noticing, however, that the average distance, determined by the gravity center of the area under the curves, coincides for both distributions. The difference between O···O

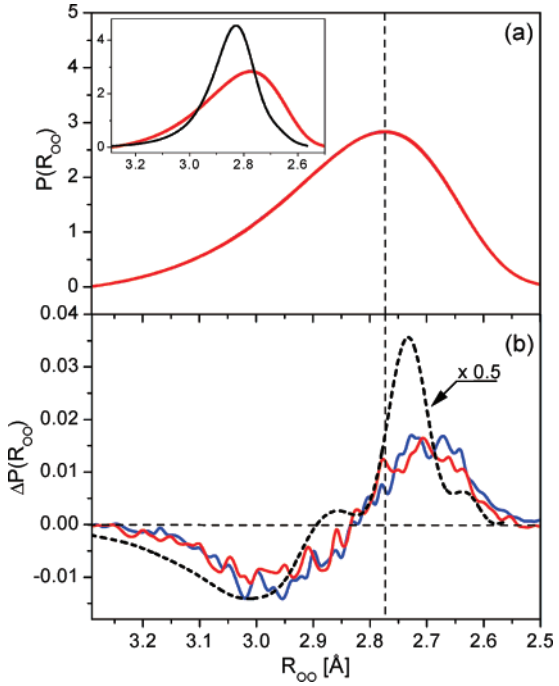

Figure 14. (a) Computed oxygen−oxygen distance distribution functions for water molecules solvating *cis*- (red) and *trans*-NMA (blue) in the first (solid) and the consecutive hydration spheres (dotted). Inset: the comparison of the distance distribution functions calculated from MD results for the third hydration sphere of the *cis*-NMA (red), treated as the bulk phase, and that for bulk water derived from the experimental infrared spectral data (black). (b) Difference between oxygen−oxygen distance distribution functions for water molecules in the first and in the third hydration sphere of the *cis*-NMA (red) and *trans*-NMA (blue) along with the respective normalized difference (see the text; multiplied by factor 0.5) for NMA-affected water and bulk water derived from the infrared spectral data (black, dotted).

distance distribution for the first hydration sphere of NMA and bulk water (considered as water from the third hydration sphere) has been visualized in Figure 14b for *trans*- and *cis*-NMA and compared with the corresponding difference of distance distribution derived from infrared spectra (Figure 8b). To better compare the experimental and simulated differences in Figure 14b, different conditions for obtaining the distribution curves have been taken into account: the NMA-affected water spectrum has been obtained for 2.9 influenced water molecules (Table 3), whereas simulation recognized 31.3 water molecules in the first hydration sphere (Table 6). Thus, the difference derived from infrared spectra has been divided in Figure 14b by the factor 31.3/2.9 (≈10.8) to obtain a more compatible result.

Agreement obtained for the course of curves in Figure 14b is unexpectedly good, deriving verified characteristics of the structural state of water molecules in NMA environment in aqueous solution. The results confirm that the O···O distance of H-bonded water molecules is shortened in the first hydration sphere of NMA, which should be a second reason for the higher energy of water H-bonds in this solute's surrounding.

Conclusions

The characteristic of hydration obtained for simple amides in aqueous solution, studied as models for basic repeating unit of polypeptides and proteins, has been obtained by various experimental and theoretical methods. The consistency of spectral studies and molecular dynamics simulations appears to be impressive in finding out the molecular details of hydration.

Water molecules in aqueous solution can efficiently compete with the proton-donor and proton-acceptor groups of amides. The hydration sphere of these solutes is a compromise between amide−water and water−water interactions. It resembles a clathrate-like cage, disordered by electrophilic interaction. Practically no orientation and energetic effects are observed outside the first hydration sphere. Generally, A-derivatives proved more hydrophobic in character than F-derivatives, and interaction of water molecules with the carbonyl group of the amide favors a stronger H-bonded lattice in the hydration sphere, whereas interaction with the amine proton has a destabilizing influence. Ab initio calculations discover that cooperative and anticooperative interactions of water molecules with electrophilic centers of a solute influence a subtle balance on the resultant water state in the hydration sphere of an amide. The NMA molecule seems to be the best model for polypeptides, because of the chemical superstructure, regardless of that it appears to be the most hydrophobic solute among the studied amides. The H-bonded lattice around this amide is reinforced relative to bulk water; the energetic effect can be estimated as ca. 8 kJ/mol of NMA. Similar behavior is expected for the repeating unit of polypeptides.

Acknowledgment. Calculations in Gaussian 03 and molecular dynamic simulations in GROMOS96 were carried out at the Academic Computer Center in Gdańsk (TASK). One of us (J.Z.) also wishes to thank to ChemBioFarm Center of Excellence for providing access to a computer for further analysis of MD results. This work was supported from the Republic of Poland scientific funds as a research project (grant no. N N204 3799 33).

References and Notes

(1) Engdahl, A.; Nelander, B.; Astrand, P. O. *J. Chem. Phys.* **1993**, *99*, 4894.
(2) Shin, S.; Kurawaki, A.; Hamada, Y.; Shinya, K.; Ohno, K.; Tohara, A.; Sato, M. *J. Mol. Struct.* **2006**, *791*, 30.
(3) Ganeshsrinivas, E.; Sathyanarayana, D. N. *J. Mol. Struct.* (*THEOCHEM*) **1996**, *361*, 217.
(4) Knudsen, R.; Sala, O.; Hase, Y. *J. Mol. Struct.* **1994**, *321*, 187.
(5) Zhang, R.; Li, H.; Lei, Y.; Han, S. *J. Mol. Struct.* **2004**, *693*, 17.
(6) Xu, Z.; Li, H.; Wang, C.; Wu, T.; Han, S. *Chem. Phys. Lett.* **2004**, *394*, 405.
(7) Nandini, G.; Sathyanarayana, D. N. *J. Mol. Struct.* (*THEOCHEM*) **2002**, *579*, 1.
(8) Radzicke, A.; Pedersen, L.; Wolfenden, R. *Biochemistry* **1988**, *27*, 4538.
(9) Zhang, R.; Li, H.; Lei, Y.; Han, S. *J. Phys. Chem. B* **2005**, *109*, 7482.
(10) Barker, R. H.; Boudreaux, G. J. *Spechtrochim. Acta* **1967**, *23A*, 727.
(11) Kang, Y. K. *J. Mol. Struct.* (*THEOCHEM*) **2001**, *546*, 183.
(12) Lovas, F. L.; Suenram, R. D.; Fraser, G. T.; Gillies, C. W.; Zoom, D. *J. Chem. Phys.* **1988**, *88*, 722.
(13) Fantoni, A. C.; Caminati, W. *J. Chem. Soc. Faraday Trans.* **1996**, *92*, 343.
(14) Fujitake, M.; Kubota, Y.; Ohashi, N. *J. Mol. Struct.* **2006**, *236*, 97.
(15) Fantoni, A. C.; Caminati, W.; Hartwig, H.; Stahl, W. *J. Mol. Struct.* **2002**, *612*, 305.
(16) Ohtaki, H.; Itoh, S.; Rhode, M. *Bull. Chem. Soc. Jpn.* **1986**, *59*, 271.
(17) Hammami, F.; Bahri, M.; Nasr, S.; Jaidane, N.; Oummezzine, M.; Cortes, R. *J. Chem. Phys.* **2003**, *119*, 4419.
(18) Kitano, M.; Kuchitsu, K. *Bull. Chem. Soc. Jpn.* **1974**, *47*, 631.
(19) Neuefeind, J.; Chieux, P.; Zeidler, M. D. *Mol. Phys.* **1992**, *76*, 143.
(20) Schultz, G.; Hargittai, I. *J. Phys. Chem.* **1993**, *97*, 4966.
(21) Kitano, M.; Kuchitsu, K. *Bull. Chem. Soc. Jpn.* **1973**, *46*, 3048.
(22) Barthel, J.; Bachhuber, K.; Buchner, R.; Gill, J. R.; Kleebauer, M. *Chem. Phys. Lett.* **1990**, *167*, 62.
(23) Barthel, J.; Buchner, R.; Wurm, B. *J. Mol. Liq.* **2002**, *98*−*99*, 51.
(24) Hinton, J. F.; Harpool, R. D. *J. Am. Chem. Soc.* **1977**, *99*, 349.
(25) Pullman, A.; Berthod, H.; Giessner-Pretre, C.; Hinton, J. F.; Harpool, D. *J. Am. Chem.* Soc. **1978**, *100*, 3991.

(26) Jasien, P. G.; Stevens, W. J. *J. Chem. Phys*. **1986**, *84*, 3271.
(27) Sobolewski, A. L. *J. Photochem. Photobiol. A: Chem*. **1995**, *89*, 89.
(28) Fu, A.; Du, D.; Zhou, Z. *J. Mol. Struct.* (*THEOCHEM*) **2003**, *623*, 315.
(29) Kupka, T.; Gerothanassis, I. P.; Demetropoulos, I. N. *J. Mol. Struct.* (*THEOCHEM*) **2000**, *531*, 143.
(30) Renugopalakrishnan, V.; Madrid, G.; Cuevas, G.; Hagler, A. T. *Proc. Indian Acad. Sci*. **2000**, *112*, 35.
(31) Contador, J. C.; Aguilar, M. A.; Sanchez, M. L.; Olivares del Valle, F. J. *J. Mol. Struct.* (*THEOCHEM*) **1994**, *314*, 229.
(32) Rablen, P. R.; Lockman, J. W.; Jorgensen, W. L. *J. Phys. Chem. A* **1998**, *102*, 3782.
(33) Kwiatkowski, J. S.; Leszczynski, J. *J. Mol. Struct*. **1993**, *297*, 277.
(34) Contador, J. C.; Sanchez, M. L.; Aguilar, M. A.; Olivares del Valle, F. J. *J. Chem. Phys*. **1996**, *104*, 5539.
(35) Parreira, R. L. T.; Valdes, H.; Galembeck, S. E. *Chem. Phys.* **2006**, *331*, 96.
(36) Sathyan, N.; Santhanam, V.; Sobhanadri, J. *J. Mol. Struct.* (*THEOCHEM*) **1995**, *333*, 179.
(37) Besley, N. A.; Hirst, J. D. *J. Am. Chem. Soc*. **1999**, *121*, 8559.
(38) Torii, H. *J. Phys. Chem. A* **2004**, *108*, 7272.
(39) Dannenberg, J. J. *J. Phys. Chem. A* **2006**, *110*, 5798.
(40) Samdal, S. *J. Mol. Struct*. **1998**, *440*, 165.
(41) Wong, M. W.; Wiberg, K. B. *J. Phys. Chem*. **1992**, *96*, 668.
(42) Ludwig, R.; Weinhold, F.; Farrar, T. C. *J. Chem. Phys*. **1997**, *107*, 499.
(43) Cordeiro, J. M. M.; Cordeiro, M. A. M.; Bosso, A. R. S. A.; Politi, J. R. S. *Chem. Phys. Lett.* **2006**, *423*, 67.
(44) Selvarengan, P.; Kolandaivel, P. G. *J. Mol. Model*. **2004**, *10*, 198.
(45) Kang, Y. K. *J. Mol. Struct.* (*THEOCHEM*) **2001**, *546*, 183.
(46) Han, W. G.; Suhai, S. *J. Phys. Chem*. **1996**, *100*, 3942.
(47) Kubelka, J.; Keiderling, T. A. *J. Phys. Chem. A* **2001**, *105*, 10922.
(48) Torri, H.; Tatsumi, T.; Tasumi, M. *J. Raman Spectrosc*. **1998**, *29*, 537.
(49) Bour, P.; Keiderling, T. A. *J. Chem. Phys*. **2003**, *119*, 11253.
(50) Kaur, D.; Kaur, R. P. *J. Mol. Struct.* (*THEOCHEM*) **2005**, *757*, 53.
(51) Desfrancois, C.; Periquet, V.; Carles, S.; Schermann, J. P.; Smith, D. M. A.; Adamowicz, L. *J. Chem. Phys*. **1999**, *110*, 4309.
(52) Xu, Z.; Li, H.; Wang, C.; Wu, T.; Han, S. *Chem. Phys. Lett*. **2004**, *394*, 405.
(53) Kang, Y. K.; Park, H. S. *J. Mol. Struct.* (*THEOCHEM*) **2004**, *676*, 171.
(54) Kulkarni, A. D.; Babu, K.; Gadre, S. R.; Bartolotti, L. J. *J. Phys. Chem.* **2004**, *108*, 2492.
(55) Mirkin, N. G.; Krimm, S. *J. Mol. Struct.* (*THEOCHEM*) **1995**, *334*, 1.
(56) Jorgensen, W. L.; Gao, J. *J. Am. Chem. Soc*. **1988**, *110*, 4212.
(57) Guo, H.; Karlplus, M. *J. Phys*. **1992**, *96*, 7273.
(58) Rocha, W. R.; De Almeida, K. J.; Coutinho, K.; Canuto, S. *Chem. Phys. Lett.* **2001**, *345*, 171.
(59) Rocha, W. R.; Martins, V. M.; Coutinho, K.; Canuto, S. *Theor. Chem. Acc*. **2002**, *108*, 31.
(60) Cordeiro, M. A. M.; Santana, W. P.; Cusinato, R.; Cordeiro, J. M. M. *J. Mol. Struct.* (*THEOCHEM*) **2006**, *759*, 159.
(61) Jorgensen, W. L.; Swenson, C. J. *J. Am. Chem. Soc.* **1985**, *107*, 1489.
(62) Krienke, H.; Foscher, R.; Barthel, J. *J. Mol. Liq*. **2002**, *98*−*99*, 329.
(63) Cordeiro, J. M. M.; Freitas, L. C. G. *Z. Naturforsch.* **1999**, *54A*, 110.
(64) Puhovski, Y. P.; Rode, B. M. *J. Chem. Phys*. **1995**, *102*, 2920.
(65) Puhovski, Y. P.; Rode, B. M. *J. Chem. Phys*. **1995**, *99*, 1566.
(66) Puhovski, Y. P.; Rode, B. M. *Chem. Phys*. **1995**, *190*, 61.
(67) Sanchez, M. L.; Aguilar, M. A.; Olivares del Valle, F. J. *J. Comput. Chem*. **1997**, *18*, 313.
(68) Chalaris, M.; Samios, J. *J. Chem. Phys*. **2000**, *112*, 8581.
(69) Arroyo, S. T.; Martin, J. A. S.; Garcia, A. H. *Chem. Phys*. **2006**, *327*, 187.
(70) Puhovski, Y. P.; Safonova, L. P.; Rode, B. M. *J. Mol. Liq*. **2003**, *103*−*104*, 15.
(71) Lei, Y.; Pan, H.; Han, S. *J. Phys. Chem. A* **2003**, *107*, 1574.
(72) Elola, M. D.; Ladanyi, B. M. *J. Chem. Phys.* **2006**, *125*, 184506.
(73) Schoester, P. C.; Zeidler, M. D.; Radnai, T.; Bopp, P. A. *Z. Naturforsch.* **1995**, *50A*, 38.
(74) Torii, H.; Tasumi, M. *J. Phys. Chem. A* **2000**, *104*, 4174.
(75) Kwac, K.; Cho, M. *J. Chem. Phys*. **2003**, *119*, 2256.
(76) Waldon, R. D. *J. Chem. Phys*. **1957**, *26*, 809.
(77) Horning, D. F. *J. Chem. Phys*. **1964**, *40*, 3119.
(78) Falk, M.; Ford, T. A. *Can. J. Chem*. **1966**, *44*, 1699.
(79) Eriksson, A.; Kristiansson, O.; Lindgren, J. *J. Mol. Struct*. **1984**, *114*, 455.
(80) Kristiansson, O.; Eriksson, A.; Lindgren, J. *Acta Chem. Scand. A* **1984**, *38*, 609, 613.
(81) Stangret, J. *Spectrosc. Lett*. **1988**, *21*, 369.
(82) Stangret, J.; Gampe, T. *J. Phys. Chem. B* **1999**, *103*, 3778.
(83) Badger, R. M.; Bauer, S. H. *J. Chem. Phys*. **1937**, *5*, 839.
(84) Gojło, E.; Gampe, T.; Krakowiak, J.; Stangret, J. *J. Phys. Chem. A* **2007**, *111*, 1827.
(85) Frisch, M. J.; Trucks, G. W.; Schlegel, H. B.; Scuseria, G. E.; Robb, M. A.; Cheeseman, J. R.; Montgomery, J. A., Jr.; Vreven, T.; Kunin, K. N.; Burant, J. C.; Millam, J. M.; Iyengar, S. S.; Tomasi, J.; Barone, V.; Mennucci, B.; Cossi, M.; Scalani, G.; Rega, N.; Petersson, G. A.; Nakatsuji, H.; Hada, M.; Ehara, M.; Toyota, K.; Fukusa, R.; Hasegawa, J.; Ishida, M.; Nakajima, T.; Honda, Y.; Kitao, O.; Nakai, H.; Klene, M.; Li, X.; Knox, J. E.; Hratchian, H. P.; Cross, J. B.; Bakken, V.; Adamo, C.; Jaramillo, J.; Gomperts, R.; Stratmann, R. E.; Yazyev, O.; Austin, A. J.; Cammi, R.; Pomelli, C.; Ochterski, J. W.; Atala, P. Y.; Morokuma, K.; Voth, G. A.; Salvador, P.; Dannenberg, J. J.; Zakrzewski, V. G.; Dapprich, S.; Daniels, A. D.; Strain, M. C.; Farkas, O.; Malick, D. K.; Rabuck, A. D.; Raghavachari, K.; Foresman, J. B.; Ortiz, J. V.; Cui, Q.; Babul, A. G.; Clifford, S.; Cioslowski, J.; Stefanom, B. B.; Liu, G.; Liashenko, A.; Piskorz, P.; Komaromi, I.; Martin, R. L.; Fox, D. J.; Keith, T.; Al-Laham, M. A.; Peng, C. Y.; Nanayakkara, A.; Challacombe, M.; Gill, P. M. W.; Johnson, B.; Chen, W.; Wong, M. W.; Gonzalez, C.; Pople, J. A. *Gaussian 03*, revision B.05; Gaussian; Inc.: Wallingford, CT, 2004.
(86) Becke, A. D. *J. Chem. Phys.* **1993**, *98*, 5648.
(87) Krishnan, R.; Binkley, J. S.; Seeger, R.; Pople, J. A. *J. Chem. Phys.* **1980**, *72*, 650.
(88) Van Gunsteren, W. F.; Billeter, S. R.; Eising, A. A.; Hünenberger, P. H.; Krüger, P.; Mark, A. E.; Scott, W. R.; Tironi, I. G. *Biomolecular Simulation: The GROMOS96 Manual and User Guide*; Biomos b. v.: Zürich, 1996.
(89) Wernet, Ph.; Nordlund, D.; Bergmann, U.; Cavalleri, M.; Odelius, M.; Ogasawara, H.; Näslund, L. Å.; Hirsch, T. K.; Ojamäe, L.; Glatzel, P.; Pettersson, L. G. M.; Nilsson, A. *Science*, **2004**, *304*, 995.
(90) Glew, D. N.; Rath, N. S. *Can. J. Chem*. **1971**, *49*, 837.
(91) Bergström, P-Å.; Lindgren, J. *J. Phys. Chem.* **1991**, *95*, 8575.
(92) Berglund, B.; Lindgren, J.; Tegenfeldt, J. *J. Mol. Struct.* **1978**, *43*, 179.
(93) Pieniążek, P. A.; Stangret, J. *Vib. Spectrosc*. **2005**, *39*, 81.
(94) Cabani, S.; Gianni, P.; Mollica, V.; Lepori, L. *J. Solution Chem.* **1989**, *10*, 563.
(95) Stangret, J. *J. Mol. Struct*. **2002**, *643*, 29.
(96) Gutmann, V. *Electrochim. Acta* **1976**, *21*, 661.
(97) Stangret, J.; Kamieńska-Piotrowicz, E. *J. Chem. Soc. Faraday Trans.* **1997**, *93*, 3463.
(98) Stangret, J.; Gampe, T. *J. Phys. Chem. A* **2002**, *106*, 5393.
(99) Modig, K.; Pfrommer, B. G.; Halle, B. *Phys. Rev. Lett*. **2003**, *90*, 075502.
(100) Maloney, M. W.; Jorgensen, W. L. *J. Chem. Phys*. **2000**, *112*, 8910.
(101) Mark, P.; Nilsson, L. *J. Phys. Chem. A* **2001**, *105*, 9954.